The study of seismic response and crack dynamic extension rule of the concrete dam under the fluid-solid coupling action

Ke Ming Sun, Moj Raj Bagale
Liaoning Technical University, Fuxin, Liaoning province P.R China
asskkmm11@163.com, bmojrajbagale@yahoo.com

Abstract

Combining with the concrete elastic damage theory, make a dynamic simulation analysis on the seismic response and crack dynamic extension rule of the concrete dam under the fluid-solid coupling action with the extended finite element technology, the conclusions are as follows: under the seismic action, tension failure and shear failure appear at the same time, shear failure happens to the side near the reservoir, stress concentration phenomenon appears at the inflection point of the dam, which lead to the tension failure and producing crack band, and the crack run through the dam to the failure of the dam; the dam crack appears when the seismic waves reach the peak value, and the change rule of displacement, velocity and stress distribution is similar to the seismic wave acceleration change curve; the failure of dam is induced by the both action of seismic and reservoir.

Keywords: damage failure; crack dynamic extension; seismic response; extended finite element; crack degree.

1. Introduction

Damage in concrete is a difficult problem because it induces localization and discontinuity in the displacement field, not only at the micro-level, but also at the meso- and macro-level. Although for a steel it is possible to identify the constitutive behavior on a meso-scale structure, assuming sufficient homogeneity in the test, concrete is strongly affected by its considerable degree of heterogeneity and only the initial elastic behavior can be identified on a meso-scale structure, without the occurrence of localization on a meso- and macro-level[1~5]. Research has been examining localization and softening problems carefully over recent years, in order to establish which models are mesh-independent in the descending branch of the constitutive relations, and evaluate their efficiency in analyzing concrete structures. De Borst, Sluys and Pamin have provided enlightening contribution to current thinking, clarifying the advantages and disadvantages of different approach and different failure modes. All the approaches introduce a characteristic length so as to avoid confining localization to zero-volume zones with the progressive reduction to zero of dissipative energy[6~11]. Now well supported by extensive computational experience for both the micro plane and Cauchy continuum formulations. The proposed model follows the non-local damage. The nature of each material movement or change of state is a thermodynamic process]. Thermodynamics of reversible process refers to the process of each step can proceed in the opposite direction but not in the external cause other changes. When the movement or change of state with energy dissipation, the thermodynamic process is irreversible. Although, all kinds of materials under different damage many manifestations, are very complex, but they are having a common characteristic: namely the injury is a need for energy dissipation of irreversible thermodynamic process. Therefore, as an injury (continuous defect field) continuum, to meet the needs of basic continuum mechanics equation (the equation of conservation of mass, momentum conservation equation, energy conservation equation).Under static load damage still occurred can be considered as a quasi static process: the process changes very slowly, so that in the limit of its every moment can be thought of as the equilibrium state[12~16].

2. Concrete dam elastic damage model

2.1 Crack detection and damaged elasticity

We assume that the fracture energy required to from a unit area of crack surface[17], G_f, is a material property.

$$G_f = \int \sigma_t du \tag{1}$$

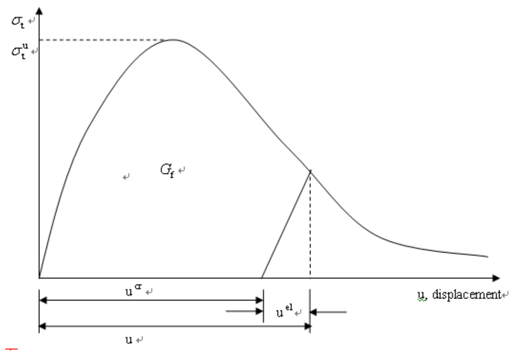

Figure 1

2.2 Strain rate decomposition

$$d\varepsilon^{el} = d\varepsilon_d^{el} + d\varepsilon_t^{pl} \tag{2}$$

where $d\varepsilon^{el}$ is the total mechanical strain rate for the crack detection problem, $d\varepsilon_d^{el}$ is the elastic strain rate, and $d\varepsilon_t^{pl}$ is the plastic strain rate associated with the crack detection surface[18].

2.3 Yield Rule

The crack detection surface is the Coulomb line

$$f_t = \hat{q} - (3 - b_0 \frac{\sigma_t}{\sigma_t^u})\hat{p} - (2 - \frac{b_0}{3}\frac{\sigma_t}{\sigma_t^u})\sigma_t = 0 \tag{3}$$

where σ_t^u is the failure stress in uniaxial tension and b_0 is a constant that is defined from the value of the tensile failure stress, σ_{I}, in a state of biaxial stress when the other nonzero principal stress, σ_{Π}, is at the uniaxial compression ultimate stress value, σ_c^u. $\sigma_t(\lambda_t)$ is a hardening parameter(σ_t is the equivalent uniaxial tensile stress)[19] .

2.4 Flow Rule

The crack detection model uses the assumption of associated flow, so if $f_t = 0$ and $d\lambda_t \rangle 0$,

$$d\varepsilon_t^{pl} = d\lambda_t \frac{\partial f_t}{\partial \sigma}; \text{ otherwise, } d\varepsilon_t^{pl} = 0 \tag{4}$$

2.5 Hardening

$$d\varepsilon_t^{pl} = d\lambda_t (\frac{3}{2}\frac{S}{q} + (1 - \frac{b_0}{3}\frac{\sigma_t}{\sigma_t^u})I) \tag{5}$$

2.6 Damaged elasticity

Following crack detection we use damaged elasticity to model the failed material. The elasticity is written in the form [20]

$$\sigma = D : \varepsilon^{el} \tag{6}$$

where D is the elastic stiffness matrix for the concrete.

2.6.1 Tension damage

$D = \dfrac{\sigma_{open}}{\varepsilon_{open}}$ Where σ_{open} is the stress corresponding to ε_{open} which is the tension stiffening.

$$\varepsilon_{open} = \max(\varepsilon^{el}) \tag{7}$$

2.6.2Shear damage

$$D = \rho G \quad \text{Where } \rho = 1 - \frac{\varepsilon^{el}}{\varepsilon_{\max}} \tag{8}$$

3. Concrete dam seismic load corresponding analysis

3.1 Project overview

In this example we consider an analysis of the Koyna dam, which was subjected to an earthquake of magnitude 6.5 on the Richter scale on December 11, 1967. The example illustrates a typical application of the concrete damaged plasticity material model for the assessment of the structural stability and damage of concrete structures subjected to arbitrary loading. The geometry of a typical non-overflow monolith of the Koyna dam is illustrated in Fig.1. The transverse and vertical components of the ground accelerations recorded during the Koyna earthquake are shown in Fig..2. (units of g = 9.81 m sec–2).

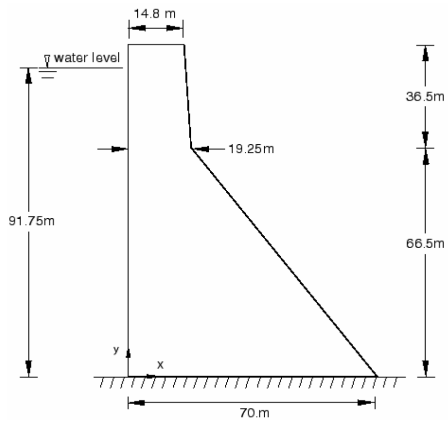

Fig.2 Geometry of the Koyna dam

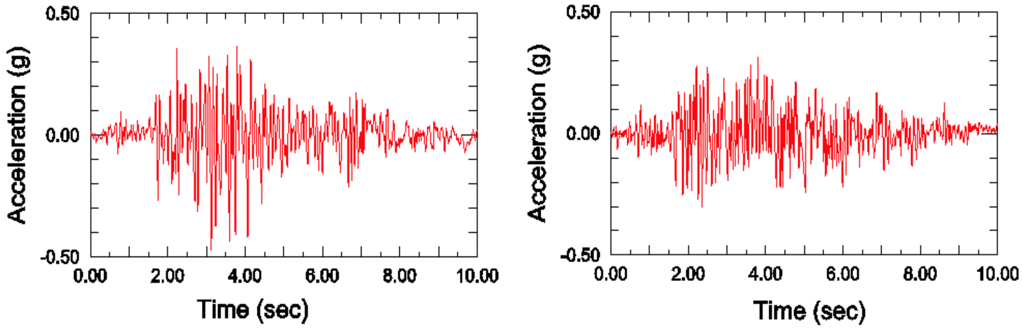

(a) transverse ground accelerations (b) vertical ground accelerations

Fig.3 Koyna earthquake accelerations

3.2 Material properties for the Koyna dam concrete

The material properties used for the simulations are given in Tab.1and Fig.4. These properties are assumed to be representative of the concrete material in the Koyna dam and are based on the properties used by previous investigators. The tensile postfailure behavior is given in terms of a fracture energy cracking criterion by specifying a stress-displacement curve instead of a stress-strain curve, as shown in Fig.4(a). Similarly, tensile damage, d_t is specified in tabular form as a function of cracking displacement, shown in Fig.4 (b). The stiffness degradation damage caused by compressive failure (crushing) of the concrete, d_c, is assumed to be zero.

Tab.1 Material properties for the Koyna dam concrete

E/MPa	υ	$\rho / kg \cdot m^{-3}$	$\psi / (^o)$	σ_{co} / MPa	σ_{cu} / MPa	σ_{to} / MPa
31027	0.15	2643	36.31	13	24.1	2.9

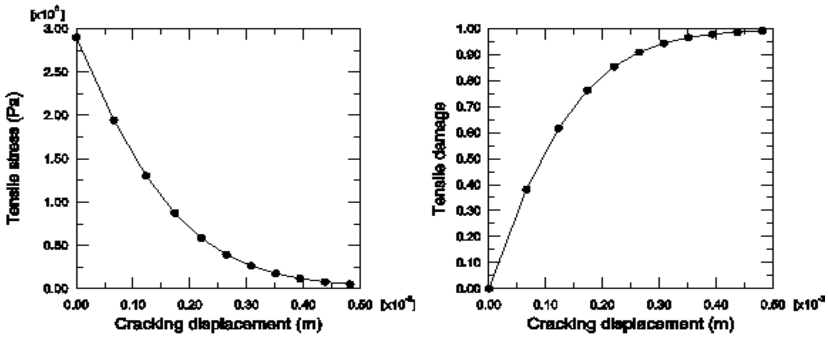

(a) tension stiffening (b) tension damage

Fig.4 Finite elements mesh of model

Calculation model with finite elements mesh is shown in Fig.4. There is the hydrostatic pressure effecting dam on the right and earthquake acting on the bottom of dam.

3.3 Results anlysis

3.3.1Free vibration analysis

The results from a frequency extraction analysis of the dam without the reservoir are summarized in Tab.2. Figure 5 shows the vibration mode analysis of dam with the natural frequency vibration.

Table.2 Natural frequencies of the Koyna dam.

Mode	Natural Frequency / (rad/sec)
1	18.86
2	49.97
3	68.16
4	98.27

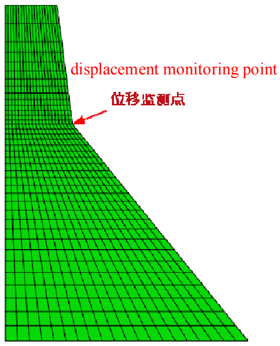

Fig.5 Finite elements mesh of model

3.3.2 Seismic analysis of the Koyna dam, not including hydrodynamic interactions

Figure 8 and Figure 9 show respectively the horizontal and vertical displacement and velocity at the left corner of the crest of the dam relative to the ground motion. In this figure positive values represent displacement in the downstream direction. The crest displacement remains less than 30 mm during the first 4 seconds of the earthquake. After 4 seconds, the amplitude of the oscillations of the crest increases substantially. As discussed below, severe damage to the structure develops during these oscillations, showed in Figure 7.

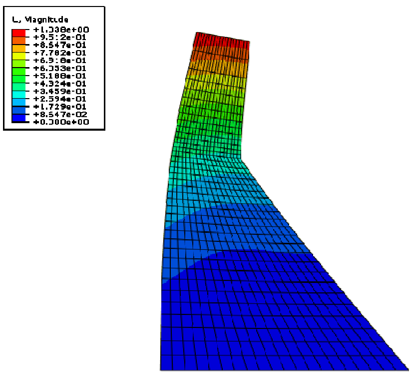

(a) First vibration mode

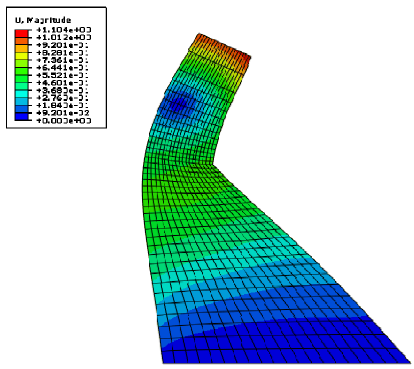

(b) Second vibration mode

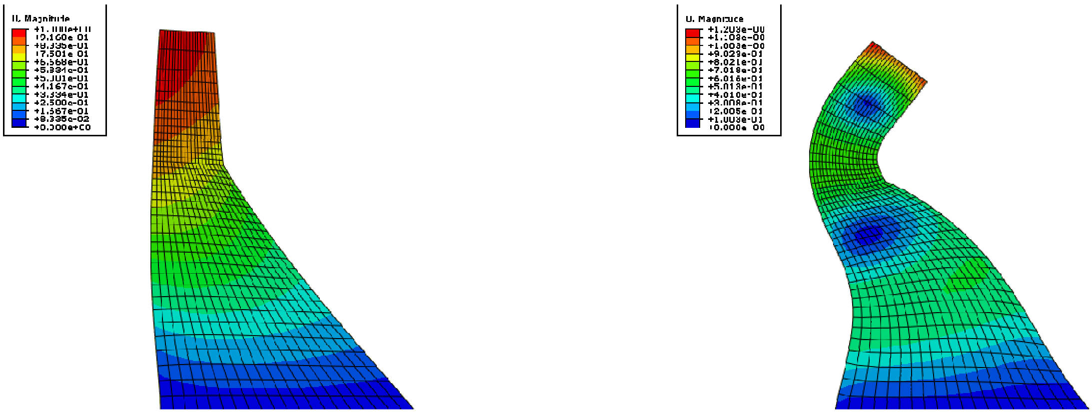

(c) Third vibration mode (d) Forth vibration mode

Fig.6 Vibration mode analysis of dam(deformation scale factor = 100)

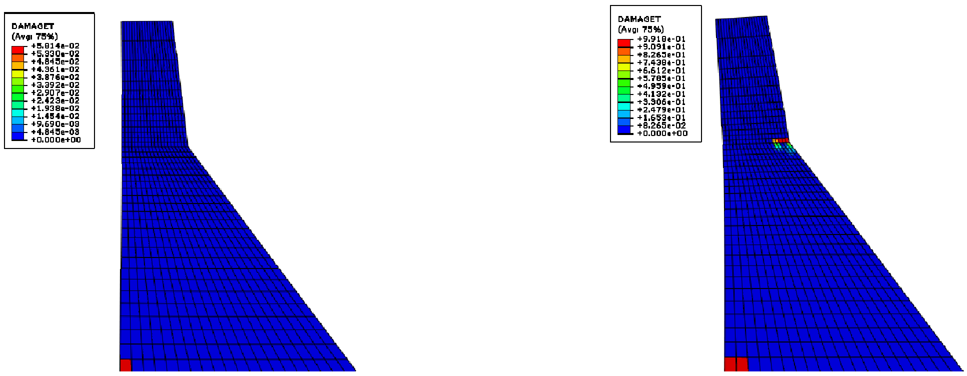

(a) t=3.271s (b) t=4.249s

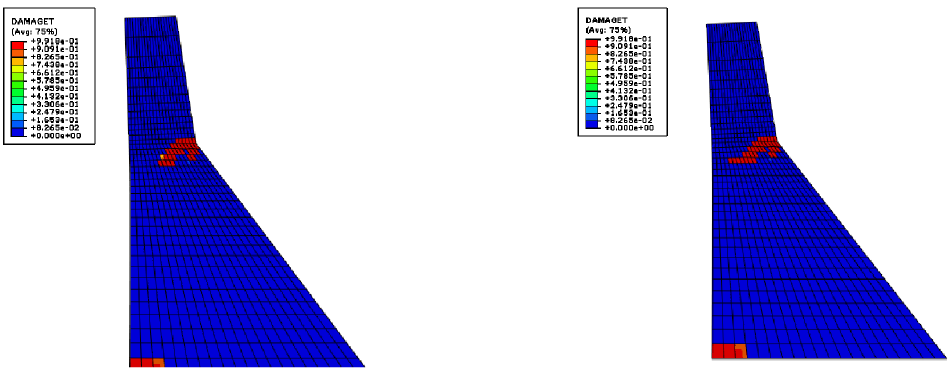

(c) t=4.709s (d) t=10s

Fig.7 Stretch induced injury of the dam(deformation scale factor = 100)

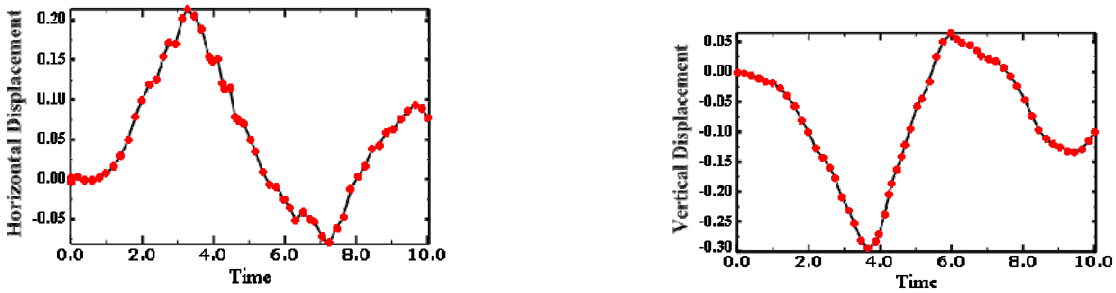

Fig.8 Monitoring point displacement curves(m)

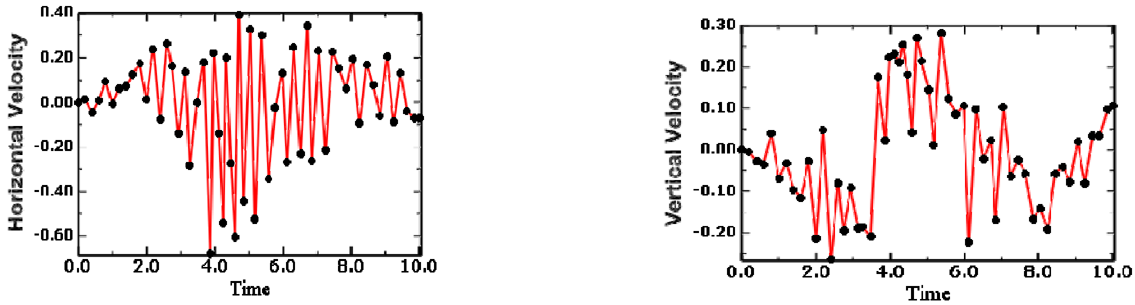

Fig.9 The dam top velocity curve(m/s)

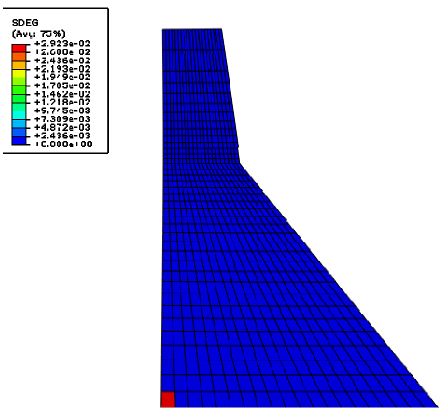

(a) t=3.271s

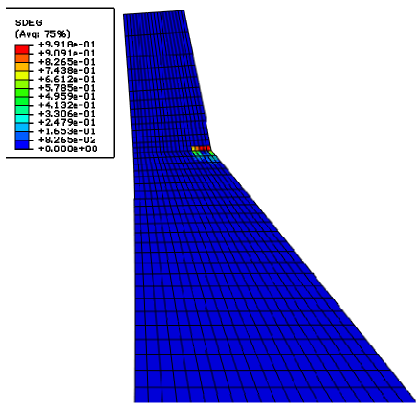

(b) t=4.249s

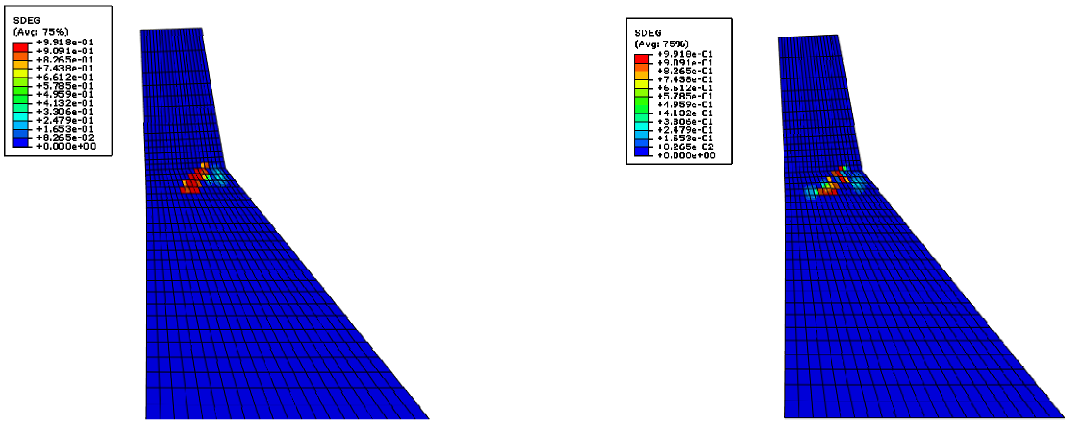

(c) t=4.709s (d) t=10s

Fig.10 The damage variable values at different times (deformation scale factor = 100)

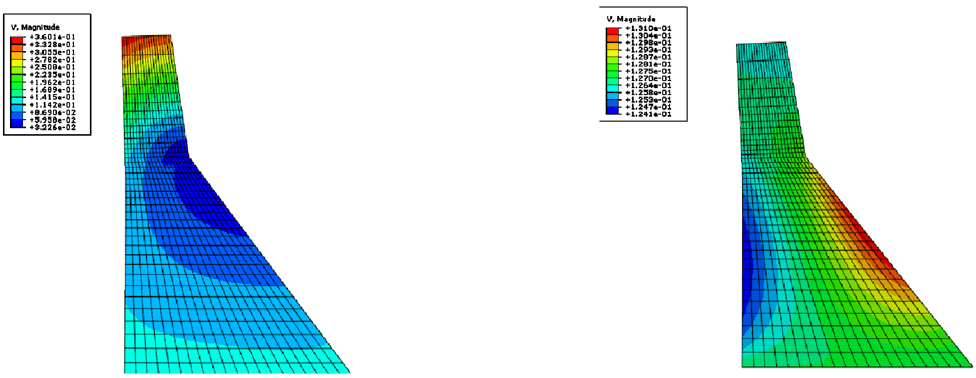

(a) t=5s (b) t=10s

Fig.11 The velocity values at different times (deformation scale factor = 100)

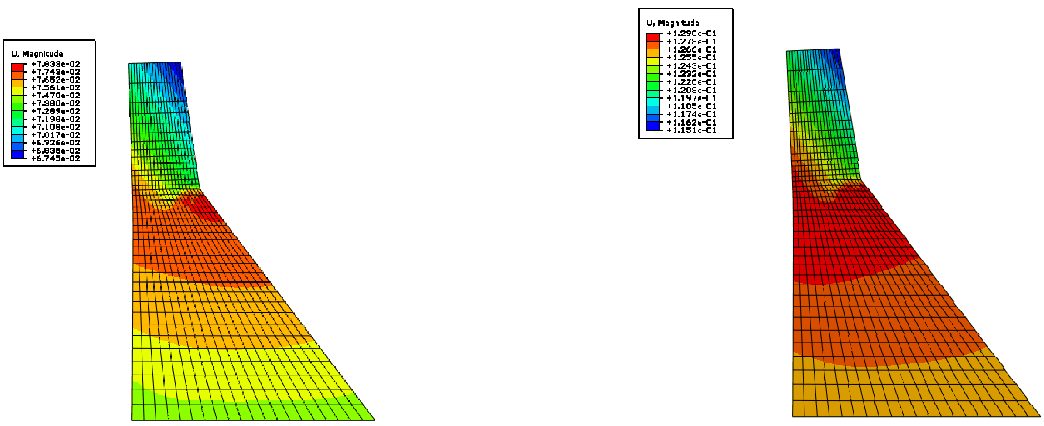

(a) t=5s (b) t=10s

Fig.12 The displacement at different times (deformation scale factor = 100)

3.3.3 Seismic analysis of the Koyna dam, including hydrodynamic interactions

Figure 13 shows the stress distribution program of dam under the action of reservoir on the left side of dam during the process of earthquake. As the graph showing, the turning points of dam appears the phenomenon of stress concentration. At the same time, the dam near the reservoir side at the bottom appears the high shear stress and shear failure is here.

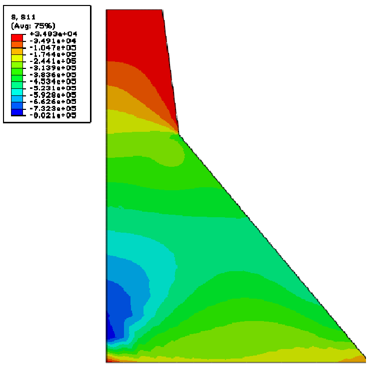

(a) stress along x direction

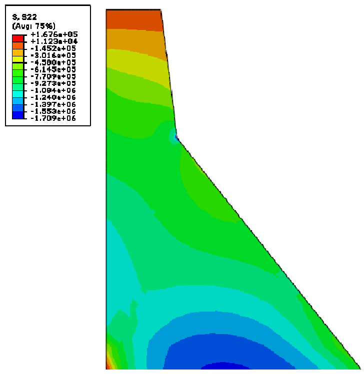

(b) stress along y direction

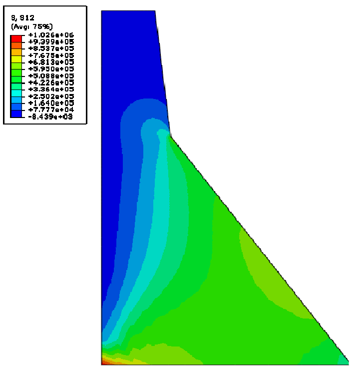

(c) shear stress

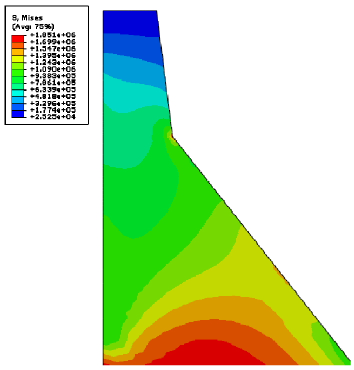

(d) mises effective stress

Fig.13 The stress distribution of dam under the action of hydrostatic pressure

In this paper, we use extended finite element technique to simulate the dynamic analysis of dam. During the seismic process, first, there appears the crack on the inflection point of dam where appears the stress concentration, which caused by tensile damage and then the crack develops as shown in figure14. What's more, we monitor the inflection point of dam in real time including the displacement, strain energy density and stress and the rules are as shown in figure 17, figure 18 and figure19. As seen from the graph, the stress, energy and displacement of the inflection point are presented the same rule, which appear the biggest amplitude when the time is fourth second during the action of earthquake. This rule is consistent with the crack dynamic change regularity showed in figure 14.

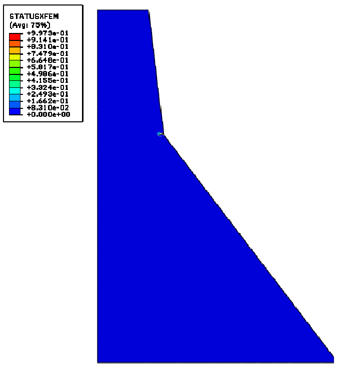

(a) t=3.876s

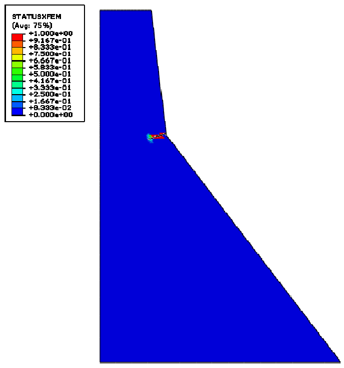

(b) t=3.886s

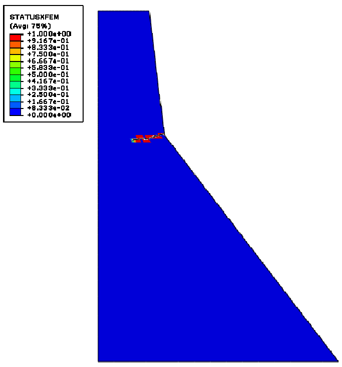

(c) t=3.96s

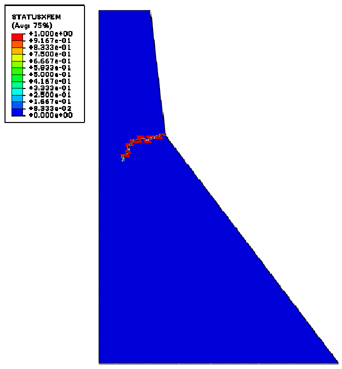

(d) t=4.33s

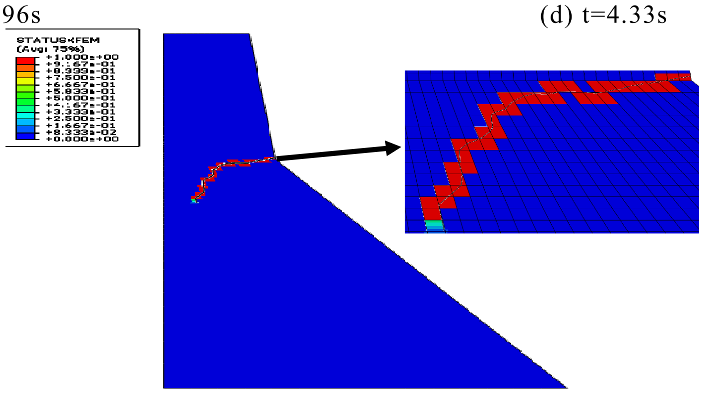

(e) t=10s

Fig.14 Status of the enriched element during the action of earthquake

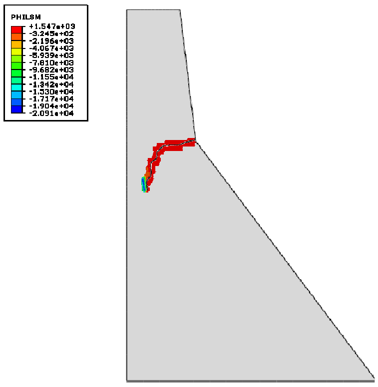

Fig.15 Signed distance function to describe the crack surface(t=10s)

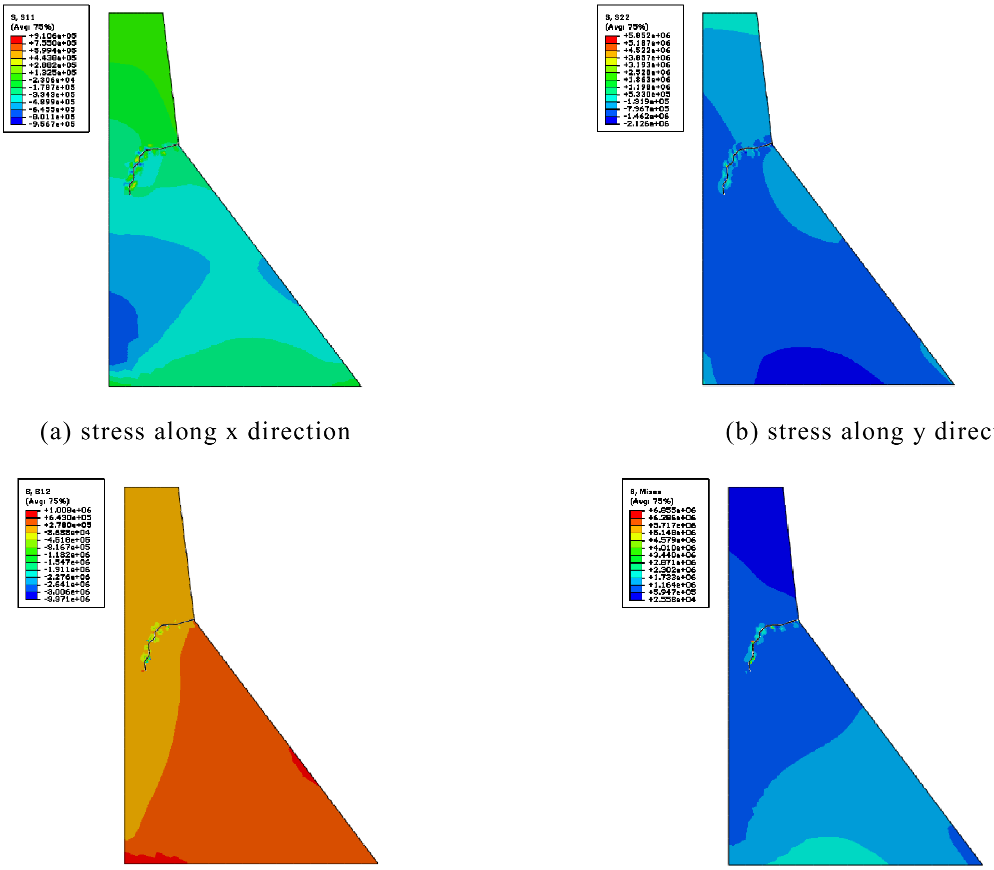

(a) stress along x direction

(b) stress along y direction

(c) shear stress

(d) mises effective stress

Fig.16 The stress distribution of dam under the action of earthquake

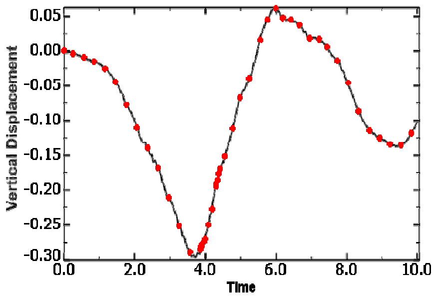

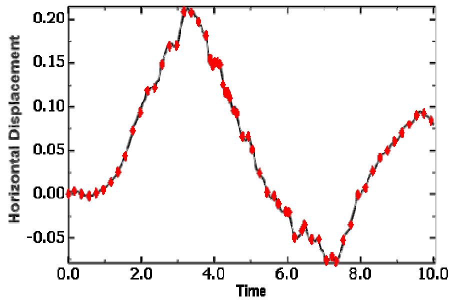

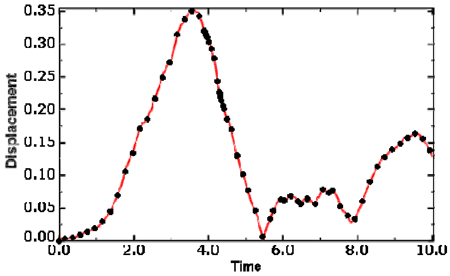

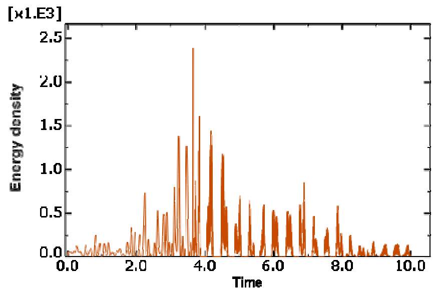

Fig.17 Dam inflection point displacement curves

Fig.18 Dam inflection point elastic strain energy density curves

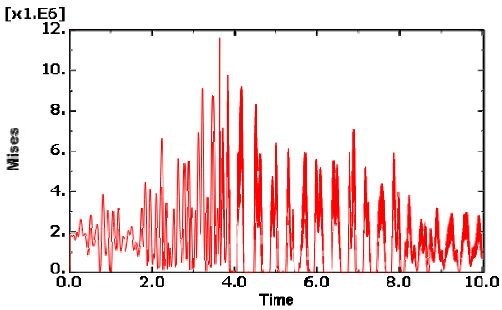

Fig.19 Dam inflection point mises effective stress curves

From the above analysis indicates that the dam final collapse is mainly composed of two parts: the first is due to dam inflection point appear stress concentration, which causing the crack appearing and further development, resulting in the complete destruction of the dam; the second is due to appear the shear failure at the bottom of dam near the reservoir side, leading to the collapse of the dam.

Conclusions

Research the earthquake response and the dynamic simulation analysis of the cracks' dynamic extension under the action of fluid-solid coupling with extended finite element technology on concrete dam body, and get the rules below:

(1) Establish the damage instability mathematical model under the coupling of seepage field and stress field of the concrete dam body;

(2) Under the action of earthquake, the tension failure and the shear failure of the concrete dam body appear at the same time. The shear failure happens on the side near the reservoir at the bottom of the dam, the shear failure belt transfer to the internal of the dam as the time elapsed. And at the same time, stress concentration phenomenon occurs at the inflexion of the dam, and tension failure happens, crack belt occurs, the two crack belts get together, which

lead to the instability and collapse of the dam;

(3) By the real-time monitoring analysis of the dam's inflexion points, we could know that the peak value of seismic wave appears when the crack appears, the crack belts appear at 4 second time at the inflexion points, the displacement, velocity, and the stress distribution of the inflexion points are familiar, are all familiar to the acceleration curve of the seismic waves;

(4) The instability and the collapse of the dam is induced by both the action of earthquake and reservoir. The damage unstable failure analysis of the dam under the action of fluid-solid coupling is more closed to the actual situation, and it has important guiding value for the dam's construction and maintenance.

References

[1] American Concrete Institute: Fracture Mechanics of Concrete: Concepts, Models and Determination of Material Properties.
[2] Technical report, American Concrete Institute (1991) Bazant, Z.P., Planas, J.: Fracture and Size Effect.
[3] CRC Press, New York (1998)178 M. Cacciola et al.
[4] Cacciola, M., La Foresta, F., Morabito, F.C., Versaci, M.: Advanced Use of Soft Computing and Eddy Current Test to Evaluate Mechanical Integrity of Metallic Plates.
[5] NDT&E International 40(5), 357–362 (2007) Morabito, F.C., Versaci, M.: A fuzzy neural approach to localizing holes in conducting plates.
[6] IEEE Transaction on Magnetics 37(5), 3534–3537 (2001)Chady, T., Enokizono, M., Takeuchi, K., Kinoshita, T., Sikora, R.: Eddy current testing of concrete structures.
[7] In: Takagi, T., Uesaka, M. (eds.) Applied Electromagnetic sand Mechanics.
[8] JSAEM Studies, pp. 509–510.
[9] IOS Press, Amsterdam (2001)
[10] Aspartic, A., Daroczi, C.S., Vertesy, G., Pavo, J.: Improvement of ECT probes based on Flux set type magnetic field sensor.
[11] In: Albanese, R., et al. (eds.) Electromagnetic Nondestructive Evaluation, vol. II, pp. 146-151.
[12] Moabite, F.C., Cockhorse, E.: A fuzzy modeling approach for the solution of an inverse electrostatic problem.
[13] IEEE Transaction on Magnetic 32(3), 1330–1333(1996)Abraham, A.: Adaptation of Fuzzy Inference System Using Neural Learning,Fuzzy System Engineering: Theory and Practice.
[14] In: Nedjah, N., et al. (eds.) Studies in Fuzziness and Soft Computing, ch. 3, pp. 53–83.
[15] Springer, Heidelberg (2005)Zadeh, L.: Fuzzy logic and its application to approximate reasoning.
[16] In: Proceedings of the Information Processing (IFIP74), pp. 591–594 (1974).
[17] Jang, R.: ANFIS: Adaptive-Network-based Fuzzy Inference Systems.
[18] IEEE Transaction on Systems, Man, and Cybernetics 23(3), 665–685 (1993).
[19] Buonsanti, M., Calking, S., Morabito, F.C., Versaci, M.: Eddy Current and Fuzzy Inference to Control Defects Growth in Reinforced Concrete.
[20] Key engineering materials, 345–346, 1291–1294 07)1231] Ross, T.J.:Fuzzy Logic with engineering applications, II edn.

Acknowledgements

Firstly, I am Moj Raj Bagale, an Author, grateful with the Chinese government for providing government scholarship for me and secondly department of engineering mechanics of Liaoning technical university for peaceful laboratory and sophisticated library with full of resources for research papers. Thirdly, I like to give thanks to highly renowned professor sun keming who always dedicated for my thesis and this paper. Lastly, I like to say thanks to my colleagues for their priceless help for me .

Thanks for natural science foundation supporting whose codes are 5087405 and 11072103.